Early Age Concrete Thermal and Creep effects: Relevance to Anchorage Zones of Post-tensioned Members

M. Sofi*
P. A. Mendis
S. Lie
Civil and Environmental Engineering Department, The University of Melbourne

D. Baweja
Cemex Australia Pty Ltd

Email: massoud@unimelb.edu.au

ABSTRACT: Highly concentrated stresses are imposed on maturing concrete slab local anchorage zones when post-tensioning (PT) load is applied. The prime nonlinear phenomena of the concrete while hydrating are the evolution of stiffness, the thermal strains, the visco-elastic nature of the concrete and cracking. Thermal and visco-elastic effects are more pronounced in early ages due to a higher rate of hydration reaction and the different phases present. The stresses associated with these effects may cause minor cracks in concrete, even prior to the application of the PT load. Finite Element simulation of early-age concrete behaviour is presented representing about four days of concrete curing in a plywood box. The thermal evolution is validated using experimental data obtained for the same mix. Results demonstrate that hydration reaction and visco-elastic effects can produce tensile stresses at critical times when the PT load is being applied. These stresses can have significant effects to the "spalling" stresses when a concentrated load is applied to the concrete section.

KEYWORDS: Anchorage zone, thermal stress, hydration reaction, early-age concrete creep.

1 INTRODUCTION

Post-tensioning of concrete slabs is a popular construction method due to the many advantages it provides. For instance, it allows faster construction pace, larger clear spans, thinner concrete slabs, and better flexibility in the spacing of columns. Large open floor areas are therefore possible, and can be achieved at a reasonable cost. These factors, combined with the ease of access to such systems, have made post-tensioning especially popular in the construction of tall buildings. In order to achieve optimum construction speed and overall economy, the floor construction cycle needs to be carefully optimized. As a part of this, it is important that post-tensioning of the slab is done as early as possible, and according to the project time schedule, so that the slab has sufficient strength when the cycle starts over for the next floor above (Cross, 2007).

To control the internal concrete stresses due to shrinkage and volume changes, an initial 25% of the total PT load is usually applied 24 hours after the concrete pour (Cross 2007). The criterion for allowing this is that the concrete must have gained a minimum compressive strength of 7MPa. When a compressive strength of 22MPa is reached 3-7 days later, the remaining post-tensioning of the slab can be carried out. The post-tensioning stress is applied using a hydraulic ram, where the stress is determined from calibrated hydraulic pressure gauges (FIB 2005). In this paper, the term 'early-age' is used to describe concrete which is one week or less in age.

1.1 *Early Age Concrete Properties*

Concrete at early ages is characterized by the fast evolution of its mechanical properties. This is due to the chemical hydration reaction occurring between the Portland cement and the water. Rate of the exothermic reaction is higher during the first few days. It slows down after three to seven days although the reaction continues well beyond 28 days.

It is important to know the strength gain and related properties of concrete during the stages when the post-tensioning load is applied. Apart from standard testing of cylinders, maturity method is often used to estimate the strength gain of the in-situ concrete. Maturity is a function of both age and temperature (Neville 1996). Maturity and hydration process are therefore highly dependent on the ambient temperatures following the casting of the fresh concrete. Accurate evaluation of the in-situ concrete strength is critical in order to avoid risk of cracking or local failure in the anchorage zone.

Important factors that may contribute to cracking and failure of the early-age concrete are the ambient conditions (e.g. temperature, humidity) and properties such as creep and shrinkage. For a restrained concrete element, creep can occur due to thermal expansion and shrinkage. Creep is considered as a time dependent deformation of concrete due to the imposed load. Immediate deformations due to applied load are referred to as the nominal elastic strains (Neville 1996). This is not completely correct since there will always be some early creep, but it is in practice good enough for most purposes. Creep can then be taken as the increase in strains as a function of time, after this point as shown in Fig.1.
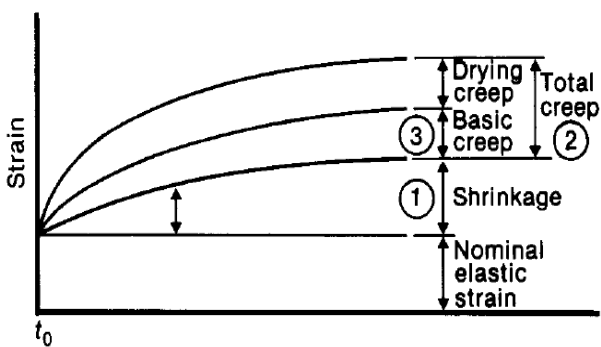

Figure 1: Time-dependent strains in concrete subjected to external loading over a time [After Neville (1996)]

Additionally, there will also be time-dependent shrinkage, unaffected of whether the concrete is loaded or not. Shrinkage is a result of chemical and physical changes in the concrete volume during the hydration process. It can be divided into plastic shrinkage and drying shrinkage. Plastic shrinkage occurs while the concrete is in the plastic phase. Drying shrinkage is mostly affected by environmental conditions such as wind speed, temperature and relative humidity. As shown in Fig. 1, there are two types of creep which can make up the total creep, depending on the moisture content of the environment. If there is no moisture movement between the concrete and the environment, it can roughly be assumed that all creep is basic creep, even though this is also a simplification.

Current design regulations rely on the compressive and tensile strength of the hydrating concrete only to estimate the anchorage zone bearing capacity. Early age effects are offset by a conservative design approach. Part of the research undertaken at the University of Melbourne is to report on the thermal and creep effects on the local anchorage zone failures. This paper presents the results of the initial stage of the study. Thermal behavior of a typical PT concrete mix hydrating in a plywood box is presented. The temperature evolution of the con-crete is validated against experimental datas. Existing creep model, Double Power Law, is adopted to investigate visco-elastic behavior. To investigate creep effects at early ages, a standard concrete cylinder is considered. The model is simulating the hydration reaction and associated thermal strains with and without consideration of the creep at early ages.

1.2 *Notes on visco-elastic behavior of early age concrete*

Elastic materials have the ability to fully regain the initial shape after being deformed. Concrete at early ages cannot be assumed to be elastic. A visco-elastic material exhibits both viscous and elastic characteristics under deformation. While elastic deformations are always recoverable upon unloading, viscous deformations are never recoverable (Neville 1996). If the magnitude of the applied load is close to the concrete strength, this would not be the case due to cracking and plastic deformations.

1.3 *Double Power Law*

The Double Power Law is the simplified version of a creep model developed by Bažant & Panula (1978). This is a widely used model for long-term creep The model has been modified by Atrushi (2003) to incorporate the visco-elasticity behaviour observed in early-age creep. This modified version of the Double Power Law is of interest to the current study.

Early age compressive and tensile creep of concrete has been investigated by Atrushi (2003) using the modified Double Power Law (DPL). Experimental laboratory tests were carried out in order to measure the creep of a set of specimens ranging from 1 to 8 days in age. The strains were then plotted along with the theoretically calculated strains estimated by the DPL. For the compressive creep, very good agreement between the two estimates was established (Fig. 3). The concrete mix, named 'BASE-5', is a high strength concrete with a water-cement ratio of 0.40 and a 28-day cylinder compressive strength of 80MPa.

The creep function, or compliance function describing the time-dependent strains is listed:

$$J(t,\tau) = \frac{1}{E(\tau)}\left[1 + \alpha\tau^{-d}(t-\tau)^p\right] \qquad (1)$$

where:

$J(t,\tau)$:   Compliance function

$E(\tau)$:   Young's modulus at the age of loading

α, d, p: Creep model parameters

τ: Age of concrete at time of loading in days

t: Age of concrete in days

Atrushi (2003) determined creep parameters by fitting the DPL curve defined by Eq. 1 to each of the experimentally obtained creep curves in Fig. 3 A and B. The parameters were then optimised and summarized into single values that best fitted all the curves. This was done for both compressive and tensile creep curves. The values are shown in Table 1.

Table 1: Optimised values for DPL creep parameters

	α	d	p
Compressive creep	0.75	0.20	0.21
Tensile creep	0.33	0.27	0.56

Faria *et al.* (2006) presented a thermo-mechanical model based on the framework of finite element with a consideration of phenomena such as the heat production due to cement hydration, evolving properties of concrete during hydration and early-age creep. Behaviour of a slab restrained by the supporting piles was successfully modelled. It was demonstrated that by making a reasonable thermal and mechanical characterization of concrete, thermo-mechanical model provides results that are well correlated to the in-situ measurements, namely the temperatures and strains.

Earlier, de Borst and van den Boogaard (1994) established the creep parameters using a curve fitting approach. The DPL was fitted to a stress development curve depicted in Fig. 4. It was reported that the stress is developed due to temperature and hydration effects. When the temperature increases, there will be thermal dilations resulting in compressive stresses up to about 80hrs. It can be seen that the measured maximum compressive stress takes place slightly later than the DPL predicts. This is not of significant concern since it is the tensile stress which is critical for cracking (de Borst & van den Boogaard 1994). The obtained values are summarised in Table 2.
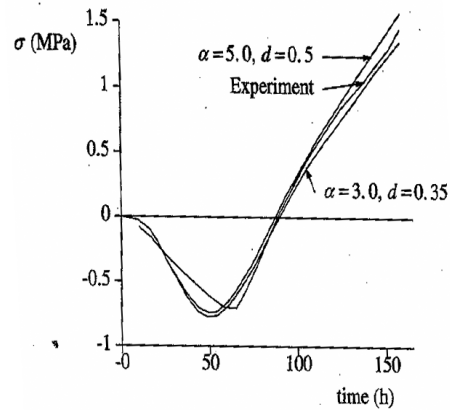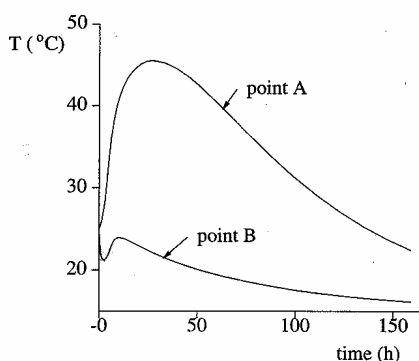
Fig. 4: Curve fitting to experimental stress development data [After de Borst & van den Boogaard (1994)]

Table 2: DPL creep material parameters

α	D	P
5.0	0.5	0.3
3.0	0.35	0.3
4.0	0.45	0.3
4.0	0.35	0.25

2 PT CONCRETE STRENGTH AND MECHANICAL PROPERTIES

The concrete mix design used in the experiment is shown in Table 3. According to preliminary tests on standardized test cylinders cured in a 20°C lime saturated water bath, it can be assumed that the compressive strength, f'_c is in the order of 40 MPa (Sofi *et al* 2008).

Fig. 5 exhibits an example of the development of the mean compressive strength (*fcm*) over time for test specimens cured under isothermal conditions and with a water-cement ratio of 0.5 (Sofi *et al* 2007).

Table 3: Concrete mix for beam [After Sofi, Mendis & Baweja (2008)]

Mix Description		Amount
Portland Cement Content	(kg/m³)	305
Fly ash content	(kg/m³)	35
Total Cementitious	(kg/m³)	340
W/C Ratio		0.5
Water Reducer	(ml/m³)	1360
Accelerator	(ml/m³)	1360
Air Entraining Agent	(ml/m³)	0
20 mm aggregate	(kg/m³)	550
14 mm aggregate	(kg/m³)	550
Washed Concrete Sand	(kg/m³)	770
Slump	(mm)	80 ± 15

The compressive strength was determined following Standard testing methods AS 1012.11. The strength is mainly dependent on water-cement ratio,

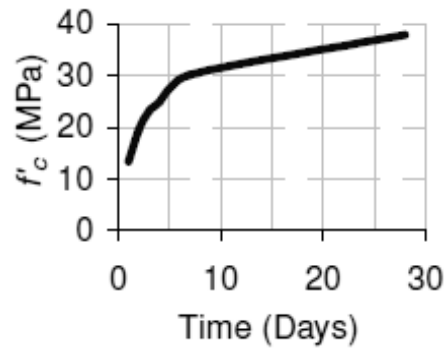type of cement used, additives, and the conditions of curing.

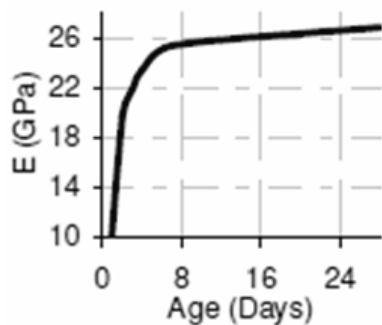Figure.5: Mean compressive strength development (f_{cm}) [After Sofi *et al* (2008)]

Figure.6 Development of modulus of elasticity over a 28-day period [After *Sofi et al* (2008)]

At early ages, the modulus of elasticity (*E*) evolves in a similar manner as the compressive strength (Fig. 6). The modulus of elasticity can be determined from compressive test specimens using a displacement gauge, or by measuring the dynamic modulus of elasticity using ultrasound (Østergaard 2003).

3 VALIDATION OF TEMPERATURE EVOLUTION CURVE

In order to simulate creep in early-age concrete using FEM program DIANA, it is necessary to simulate the temperature effects of hydration. DIANA calculates a temperature evolution curve over a chosen time period, using a number of input parameters for thermal properties of concrete. When this has been determined, stresses and strains can also be simulated, based on the temperature graph. It is therefore crucial for the accuracy of the later creep simulations that correct thermal properties of concrete are applied.

A finite element model of a beam section was used to determine the thermal parameters for input in DIANA (Fig. 7). The model is based on an actual concrete beam section that was experimentally tested (Sofi *et al.* 2007; Sofi, *et al* 2008). Prior to

the concrete pour, temperature sensors were placed in the beam. These were used to monitor the internal temperature of the beam, to be able plot graphs of the temperature evolution during the first week of hydration. Similarly, the room temperature was monitored to plot the ambient temperature.
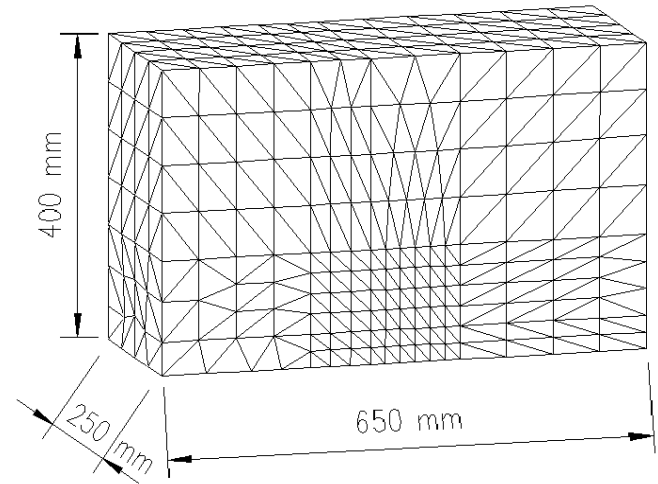

Figure 7: Finite element model of beam section

Node number 1469 shown in Fig. 8 represents the approximate position of a chosen temperature sensor set up in the beam. The sensor gives more representative temperature readings than other sensors mounted close to the surface as they may be heavily influenced by the surface convection of the concrete beam. The finite element model has elements for potential flow analysis at all boundaries. These are necessary in order to simulate the surface convection for concrete to air and concrete to formwork. For further details about the temperature validation and experimental data reference should be made to (Sofi *et al* 2007).
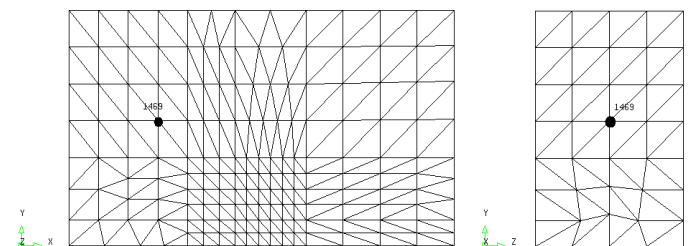

Figure 8: Node representing temperature sensor used in laboratory experiment

Instead of assuming a constant ambient temperature for the finite element model, the recorded room temperature from the experiment was used as input. The temperature predicted is very similar to the experimental data, although the model predicts a faster drop in temperature after the initial peak (Fig. 9). By changing the capacitance and surface convection, mainly the maximum temperature was affected without any effects on the shape of the curve. For

the value of thermal conductivity of concrete, very different values have been suggested, in the range of 2-8 *W/mK* (Østergaard 2003). However, more recent research proposes that the thermal conductivity of concrete decreases as the concrete matures (Gibbon & Ballim 1998). The value depends on the moisture content and temperature evolution, as well as the type of cement and aggregate of the concrete mix. It is therefore very difficult to achieve a perfectly matching curve given the non-linearities in the materials properties and the ambient conditions at the same time. In the current analysis, a linear relationship between the two values was applied to achieve the best results. The simulation results plotted against the actual temperature measurements are presented in Fig. 9.
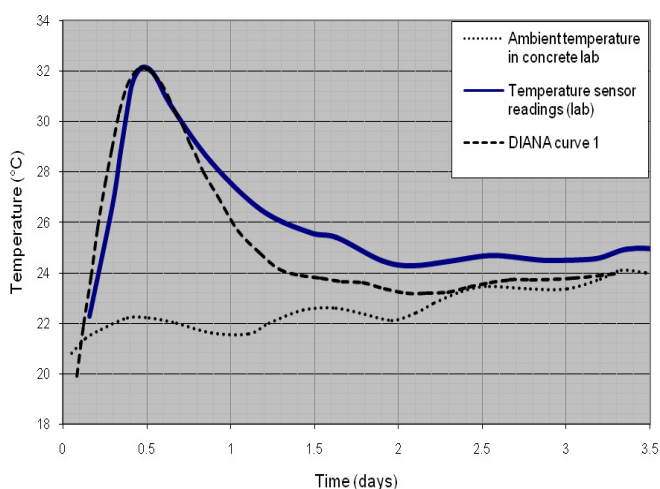

Figure 9: Temperature evolution graph obtained from DIANA and lab measurements data

To simplify the input of DIANA, the ambient temperature was assumed to be constant at 23°C. The thermal properties remained unchanged during the analyses. 'DIANA curve 2' shown in Fig.10 is the temperature evolution based on this assumption.
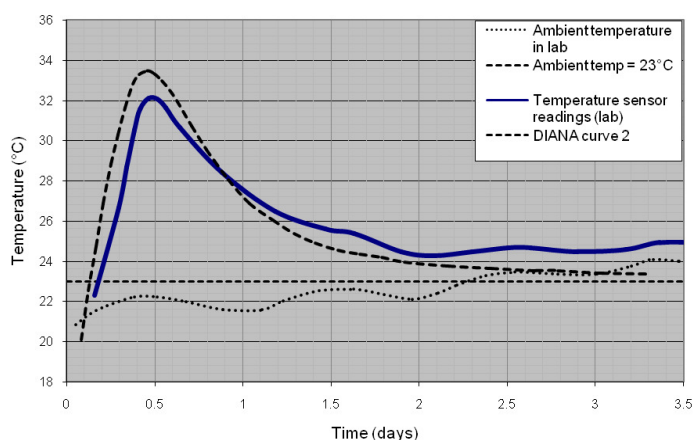

Figure 10: Temperature prediction by DIANA, ambient temperatures and lab readings

The results demonstrate that the model gives reasonable temperature predictions, using the thermal parameters stated above. The difference observed at the start of the curves can be explained by the ambient temperature in the laboratory which started at about 20°C. There were further uncertainties with regard to the specific heat capacity, which was suggested to rely on the concrete mix, moisture content, as well as the concrete temperature itself. The value has been taken as a constant in this study.

3.1 *Temperature evolution curve of typical cylinder*

Applying the thermal and material parameters determined using the beam model, the temperature time-history shown in Fig. 11 is obtained for the cylinder. The maximum temperature being reached at the centre of the cylinder is 29°C. Comparing this to the curve obtained for the beam model (Fig. 10), the maximum temperature is 3-4 degrees less for the cylinder, and the temperature falls much quicker. This is reasonable As the cylinder will loose much more heat to the surroundings because of the relatively large surface area and small thickness compared to the beam.
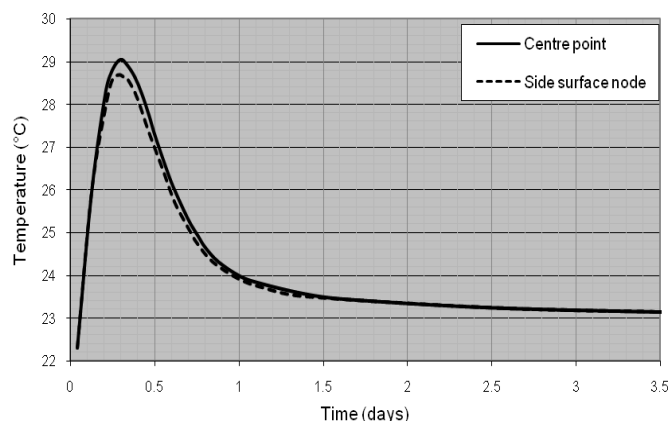

Figure 11: Temperature prediction by DIANA, ambient temperatures and lab readings

Figure 11 includes the temperature plot for two different nodes. A slightly lower temperature can be measured at node 33, located at the middle of the surface as displayed in Fig. 12. It also shows the temperature levels on the surface at the time when the maximum temperature was reached, i.e. after 7 hours.

The difference in temperature between the points demonstrates the correct heat flow characteristics of the model and the fact that the surface elements have correctly been attached to the solid elements.

3.2 *Thermal stresses excluding creep effects*

The graph presented in Fig. 12 shows the stress development caused by heat production, with stress direction along the Z-axis (from top to bottom). However, the differences between the normal directions

are negligible for a small element as the cylinder. This would for instance be more significant for the beam model used during the temperature curve validation. To obtain the stress evolution, a nonlinear structural analysis was executed taking temperature (presented in Fig.11) into account No creep model was incorporated in this analysis, in order to obtain a basis for later comparing with creep models. A heavy reliance on the temperature can be seen in that the curve shape is a mirror image of the temperature evolution curve (Fig. 11). The negative values represent the compressive stress up to 4 days age. It is demonstrated that the peak compressive stress occur at the time when the temperature reaches its maximum.
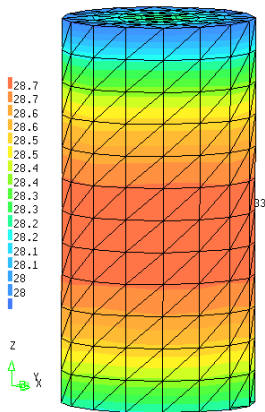

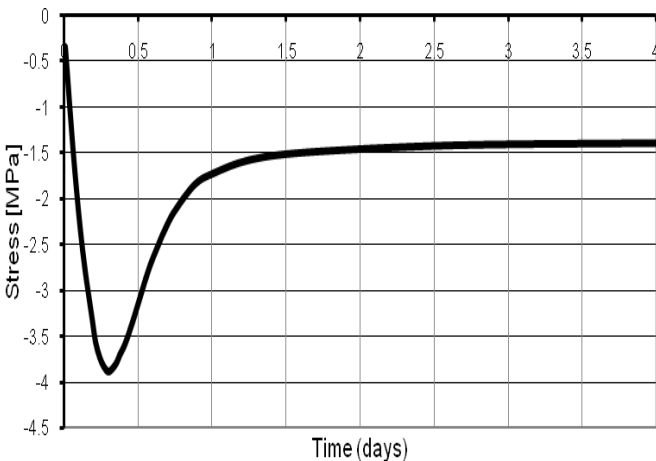Figure 11: Temperature distribution on surface of cylinder (°C)

Figure 12: Stress-time plot with creep excluded

To validate the stress-time plot a number of assumptions are made. To verify the results presented in Fig 12, heavy reliance is made on the work presented by Faria *et al.* (2006).

4 STRESS PREDICTION BY DOUBLE POWER LAW

For the application of the DPL to the current study a number of assumptions are made. The material pa-

rameters α, d and p were chosen based on the three reference papers described earlier (Atrushi 2003; de Borst & van den Boogaard 1994; Faria et al 2006). For the parameters d and p, respective values of 0.35 and 0.30 were chosen, as these agreed well with all three authors, i.e., regardless of the mixes presented. A great deal of variability is observed in the literature when considering the α-value. Atrushi (2003) suggested the values at 0.33 and 0.75. However, Atrushi based the parameters on creep deformation curves due to applied loads, whilst the other authors were looking at thermal stresses, which therefore may be more relevant for this study. Faria et al (2006) stated an α-value of 2.26, and de Borst & van den Boogaard (1994) different values from 3 to 5.

A parametric study of the α-value is presented in Figure 13. lower value of α seems to yield higher compressive stress and a delayed tensile stress at 2 days. As the value of parameter a increases, the occurrence of the tensile stress happen at a much earlier date even with a reduced prediction of the compressive stress.
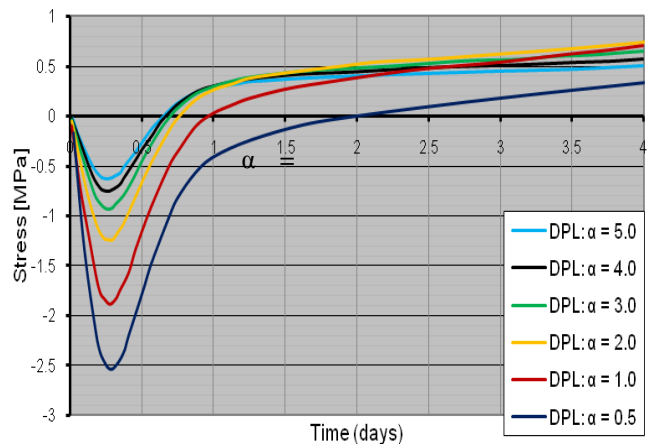

Figure 13: Stress evolution obtained from DIANA, using the Double Power Law (DPL)

Even though the compressive stress level reaches a seemingly inconsequential value of 0.5 to 1MPa, this can add to the tensile and spalling stresses occurring as a result of the PT load at the anchorage zones.

5 RELEVANCE TO THE POST-TENSIONING OF CONCRETE SLABS

As stated earlier, the post-tensioning load is applied at two stages. These correspond at times when the concrete mix is experiencing hydration reaction and heat development. To prevent unexpected failures at the local anchorage zones intrinsic stresses such as thermal and time dependent visco-elastic effects need to be considered. The design methods for post-

tensioning in the current codes of practice rely on material properties such as compressive and tensile strengths (see for e.g., AS3600) with only a marginal factor of safety other early age effects. The results presented in this paper demonstrate that tensile stresses resulting from thermal and creep effects can happen at critical times when the post-tensioning load is due to be applied (i.e., at 1-2 days) after the concrete member is cast. The current presentation relies on a cylinder model which does not represent the anchor zone stresses. However, the concrete material behavior and the imposed stresses are expected to be similar for a post-tensioned member. Although the stress levels in the cylinder are quite small, these are expected be somewhat amplified in the case of much larger members such as slabs.

6 CONCLUSIONS

Important properties of young hardening concrete have been investigated using finite elements. The obtained results correspond to findings in related literature, where pronounced effects on the stress development due to early-age creep were observed. However, more tensile stress was expected to be seen during the cooling phase. This may be explained by that the model is relatively small compared to a full-scale model of a slab section, and therefore does not result in the same build-up of stresses. Factors as mix design and strength properties of the concrete may also be of significance.

The paper attempts to presents a discussion of the early age creep effects on post-tensioning anchorage zone relying on a concrete cylinder model. It falls short of presenting stresses in the actual anchor zones of a post-tensioned member. This will form the basis of a follow up study. It is proposed that consideration of visoc-elastic effects is very important for applications such as transfer of post-tensioning loads where highly concentrated stresses are imposed on the post-tensioned member section. It is demonstrated that creep at early ages can be the basis for intrinsic tensile stresses within the concrete. Depending on the definition of the material parameters, the tensile stresses can be significant and happen at critical times when the post-tensioning load is applied.

REFERENCES

[1] Altoubat, SA & Lange, DA 2001, 'Tensile Basic Creep: Measurements and Behaviour at Early Age', ACI Materials Journal, vol. 98, no. 5, pp. 386-93.

[2] AS 1012.9 (1999) Methods of testing concrete - determination of compressive strength of concrete specimens, Australian Standard, Australia.

[3] AS 1012.17 (1997), Methods of testing concrete – Determination of the static chord modulus of elasticity and Poisson's ratio of concrete specimen, Committee BD-042, Australian Standards.

[4] AS 3600, Concrete structures, Committee BD-002, Australian Standards (2001).

[5] Atrushi, DS 2003, 'Tensile and Compressive Creep of Early Age Concrete: Testing and Modelling', Doctoral thesis, The Norwegian University of Science and Technology.

[6] Bažant, ZP & Panula, L 1978, 'Practical prediction of time dependent deformations of concrete', Materials and Structures, vol. 11, no. 65, pp. 307-28.

[7] Bissonnette, B & Pigeon, M 1995, 'Tensile creep at early ages of ordinary, silica fume and fiber reinforced concretes', Cement and Concrete Research, vol. 25, no. 5, pp. 1075-85.

[8] Cross, E 2007, 'Post-tensioning in building structures', Concrete in Australia, vol. 33, no. 4, pp. 48-54.

[9] de Borst, R & van den Boogaard, AH 1994, 'Finite-Element Modelling of Deformation and Cracking in Early-Age Concrete', ASCE Engineering Mechanics, vol. 120, no. 12, pp. 2519-34.

[10] Faria, R, Azenha, M & Figueiras, JA 2006, 'Modelling of concrete at early ages: Application to an externally restrained slab', Cement and Concrete Composites, vol. 28, pp. 572-85.

[11] FIB - Féd. Int. du Béton 2005, Post-tensioning in Buildings: Technical Report, CEB-FIP.

[12] Gibbon, GJ & Ballim, Y 1998, 'Determination of the thermal conductivity of concrete during the early stages of hydration', Magazine of Concrete Research, vol. 50, no. 3, pp. 229-35.

[13] Neville, AM 1996, Properties of Concrete, 4th and final edn, Wiley, Harlow, Essex.

[14] Østergaard, L 2003, 'Early-age fracture mechanics and cracking of concrete', Ph.D. thesis, Technical University of Denmark.

[15] Østergaard, L, Lange, DA, Altoubat, SA & Stang, H 2001, 'Tensile basic creep of early-age concrete under constant load', Cement and Concrete Research, vol. 31, no. 12, pp. 1895-9.

[16] Sofi, M, Bawa, D, Mendis, PA & Mak, SL 2007, 'Behaviour of Post-Tensioning Anchors In Early-Age Concrete Slabs', Proceedings of theThe 23rd biennial conference of the Concrete Institute of Australia, Adelaide, Australia.

[17] Sofi, M, Mendis, P & Baweja, D 2008, 'Behaviour of post-tensioning anchorage zones in early age concrete: Experimental Study', in Proceedings of the Australasian Conference on Mechanics of Solids and Materials (ACMSM), University of Southern Queensland, Toowoomba, Australia.

[18] TNO DIANA BV 2008, DIANA User's Manual - Release 9.3.

[19] Westman, G 1995, 'Basic creep and relaxation of young concrete', in R Springenschmid (ed.), Thermal Cracking in Concrete at Early Ages, Munich.